AGU PUBLICATIONS
JGR
Journal of Geophysical Research: Atmospheres

RESEARCH ARTICLE
10.1002/2015JD023608

Key Points:
- Dust concentration and size are analyzed in the EDML ice core
- Seasonal phase lag between dust concentration and size changes over Termination 1
- Major atmospheric change over Antarctica likely around 16,000 years B.P.

Correspondence to:
A. Wegner,
anna.wegner@awi.de

Citation:
Wegner, A., H. Fischer, B. Delmonte, J.-R. Petit, T. Erhardt, U. Ruth, A. Svensson, B. Vinther, and H. Miller (2015), The role of seasonality of mineral dust concentration and size on glacial/interglacial dust changes in the EPICA Dronning Maud Land ice core, *J. Geophys. Res. Atmos.*, *120*, 9916–9931, doi:10.1002/2015JD023608.

Received 29 APR 2015
Accepted 23 AUG 2015
Accepted article online 27 AUG 2015
Published online 5 OCT 2015

The role of seasonality of mineral dust concentration and size on glacial/interglacial dust changes in the EPICA Dronning Maud Land ice core

Anna Wegner[1], Hubertus Fischer[2], Barbara Delmonte[3], Jean-Robert Petit[4], Tobias Erhardt[2], Urs Ruth[1,5], Anders Svensson[6], Bo Vinther[6], and Heinrich Miller[1]

[1]Alfred Wegener Institut Bremerhaven, Helmholtz-Zentrum für Polar- und Meeresforschung, Bremerhaven, Germany, [2]Climate and Environmental Physics, Physics Institute, and Oeschger Centre for Climate Change Research, University of Bern, Bern, Switzerland, [3]Department Environmental Sciences, University Milano Bicocca, Milan, Italy, [4]Laboratoire de Glaciologie et Géophysique de l'Environnement, CNRS-Université Joseph Fourier, St. Martin d'Hères, France, [5]Robert Bosch GmbH, Corporate Sector Research and Advance Engineering, Renningen, Germany, [6]Centre for Ice and Climate, Niels Bohr Institute, University of Copenhagen, Copenhagen, Denmark

Abstract We present a record of particulate dust concentration and size distribution in subannual resolution measured on the European Project for Ice Coring in Antarctica (EPICA) Dronning Maud Land (EDML) ice core drilled in the Atlantic sector of the East Antarctic plateau. The record reaches from present day back to the penultimate glacial until 145,000 years B.P. with subannual resolution from 60,000 years B.P. to the present. Mean dust concentrations are a factor of 46 higher during the glacial (~850–4600 ng/mL) compared to the Holocene (~16–112 ng/mL) with slightly smaller dust particles during the glacial compared to the Holocene and with an absolute minimum in the dust size at 16,000 years B.P. The changes in dust concentration are mainly attributed to changes in source conditions in southern South America. An increase in the modal value of the dust size suggests that at 16,000 years B.P. a major change in atmospheric circulation apparently allowed more direct transport of dust particles to the EDML drill site. We find a clear in-phase relation of the seasonal variation in dust mass concentration and dust size during the glacial (r(conc,size) = 0.8) but no clear phase relationship during the Holocene ($0 < r(\text{conc,size}) < 0.4$). With a simple conceptual 1-D model describing the transport of the dust to the ice sheet using the size as an indicator for transport intensity, we find that the effect of the changes in the seasonality of the source emission strength and the transport intensity on the dust decrease over Transition 1 can significantly contribute to the large decrease of dust concentration from the glacial to the Holocene.

1. Introduction

Since Antarctica is covered to 98% by ice, the aeolian dust deposited on the Antarctic ice sheet is almost solely of remote origin and was transported thousands of kilometers in the atmosphere. Accordingly, mineral dust measured in Antarctic ice cores presents a unique archive to reconstruct the aeolian mineral dust load in the Southern Ocean region and atmospheric dust transport to Antarctica during the past up to 800,000 years [*Lambert et al.*, 2008, 2012]. Previous studies showed that the dust concentration in the ice cores from the East Antarctic plateau (EAP) changes on glacial-interglacial timescales by a factor of approximately 50 [e.g., *Fischer et al.*, 2007a, *Lambert et al.*, 2008; *Delmonte et al.*, 2008; *Petit et al.*, 1999], with significant impact on the radiative balance of the Earth at least on a regional scale [e.g., *Mahowald and Kiehl*, 2003].

The dust concentration in ice cores is influenced by the conditions at the source, where the dust particles are uplifted into the atmosphere, by the transport processes through the atmosphere from the source to the ice sheet and by deposition processes onto the snow surface. However, the contribution of each of these factors to the overall glacial-interglacial change is not sufficiently quantified, although different explanations are put forward [e.g., *Petit and Delmonte*, 2009, *Fischer et al.*, 2007a] as summarized in section 4. Moreover, dust-enabled atmospheric circulation models still fail to reproduce the large glacial-interglacial amplitudes in dust concentration variability in Antarctic ice cores by 1 order of magnitude [e.g., *Mahowald et al.*, 2011].

Due to the purity of the ice and the small amount of sample available, the measurement of dust characteristics is challenging; thus, most of the studies are based on samples with a resolution of several years or

decades. However, the seasonal variability of dust input to Antarctica is highly variable and a different seasonal timing of source emissions and transport intensity may play a significant role also in the observed long-term changes and cannot be assessed with multiyear averages. Dust plumes originating from South America were found in Antarctica within 6–10 days after the dust emission event [*Gasso et al*., 2010]. But dust transported in the high troposphere can have a much longer transport time to Antarctica. Due to the relatively short lifetime of mineral dust aerosol of a few days to weeks, maximum dust concentrations in Antarctica can only be encountered when strong source emissions and efficient transport work together seasonally. There are few studies dealing with dust concentration records in seasonal resolution providing information on the seasonal dust concentration maximum. These studies do not give a consistent picture for the whole Antarctic continent. *Bory et al*. [2010], find a maximum in dust concentration in spring/summer on top of Berkner Island. At Law Dome, elevated concentrations were found in spring and autumn with a minimum in winter [*Burn-Nunes et al*., 2011]. At the northern tip of the Antarctic Peninsula on James Ross Island, concentrations in aluminosilicate dust levels are highest during late winter [*McConnell et al*., 2007]. Again, aerosol measurements at South Pole show a dust concentration peak in austral summer [*Tuncel et al*., 1989]. Model results of seasonal dust input to all Antarctic sites suggest a maximum in summer for current climate conditions [*Albani et al*., 2012b]. These discrepancies indicate that models seem not to capture the seasonality of the dust maximum very well at all Antarctic sites and that the dust maxima do not occur synchronously over the whole Antarctic continent. Dust sources, the dynamics of the transport and processes en route can differ significantly within Antarctica, especially between lower altitude coastal sites and sites on the EAP.

The predominant dust source for the interior EAP during glacial times is southern South America with possible inputs from additional sources during the dusty glacials [e.g., *Delmonte et al*., 2008, 2010; *Marino et al*., 2009]. During the Holocene, other sources like Australia might become relatively more important in the Indian sector of the EAP [e.g., *Revel-Rolland et al*., 2006], whereas in the Atlantic sector the influence of Australian dust is minor [*Wegner et al*., 2012]. At the present day the emission strength of the South American source is highly variable but shows a maximum in summer [*Johnson et al*., 2010]. Also, the highest frequency of dust storms in Australia occurs in spring to summer [*Ekström et al*., 2004].

Additional information primarily on dust transport and deposition may be derived from size distribution measurements on Antarctic ice cores. Assuming a relatively constant dust size during the dust emission at the source [*Kok*, 2011], the dust size in the airborne mineral dust aerosol is mainly influenced by the size-fractionating dry deposition en route and, thus, by the length of the transport time as well as transport pathways and therewith atmospheric conditions. But size fractionation during the deposition process over the ice sheet may also influence the size distribution in polar ice [*Unnerstad and Hansson*, 2001]. The longest record of dust size from the European Project for Ice Coring in Antarctica (EPICA) Dome C ice core and the record from Komsomolskaya ice core revealed smaller sizes during cold stages [*Lambert et al*., 2008; *Delmonte et al*., 2004]. This was tentatively explained by changes in the contributions of dust transported over different pathways, larger particles transported by advection in lower altitudes and smaller particles transported in higher altitudes via subsidence [*Lambert et al*., 2008; *Delmonte et al*., 2004]. At Dome C also a slight decrease could be observed in the early deglaciation until 16,000 years B.P. In the Dome B ice core the dust size record shows the opposite glacial/interglacial trend with significantly larger dust particles during the glacial, which could be explained by regional atmospheric circulation changes over Antarctica [*Delmonte et al*., 2004].

For previous Antarctic ice core studies no consideration has been made that the size distribution of the dust deposited on the ice sheet is not only dependent on the size distribution in the overlying atmosphere (this size distribution is controlled by transport intensity) but that also the ratio of wet versus dry deposition at the site can have an influence on the size of the dust deposited on the ice sheet. Generally, it is assumed that wet deposition is at first order not size fractionating, while dry deposition velocity by gravitational settling assuming Stokes settling is dependent on the diameter squared of the dust particles. However, precipitation still has an effect on the size distribution of the deposited aerosol because the amount of wet-deposited aerosol is diluting the contribution of the size-fractionating dry deposition. In essence, the dust aerosol deposited on the ice sheet is shifted to larger particles than the overlying atmospheric aerosol by dry deposition; however, the shift decreases with increasing precipitation rate and hence with the amount of wet deposition of mineral dust. Thus, changes in precipitation rate, as parametrized by the accumulation rate in ice cores, from one climatic condition to another may have an impact on the size distribution of the dust in the ice, which might add to or compensate for the transport time effect. For the EAP, most of the deep drilling ice

core sites have lower accumulation rates than at Dronning Maud Land (DML). Thus, an effect by wet deposition might contribute more strongly in DML, whereas at sites with even lower accumulation rate wet deposition plays an even smaller role.

Seasonal variations in dust size distribution have yet not been derived from Antarctic ice cores yet. Here we fill this gap with dust size measurements on the EPICA ice core drilled in DML. Within EPICA two deep ice cores were drilled. The ice core drilled in DML (EPICA Dronning Maud Land (EDML): 75°00′S, 00°04′E, 2882 m above sea level, [*EPICA-community members*, 2006]) has a 2–3 times higher accumulation rate than the one at Dome C (EDC: 75°06′S, 123°21′E, 3233 m above sea level, [*EPICA-community members*, 2004]) and therefore provides higher resolution records down to Marine Isotope Stage 4. Moreover, it is located in the Atlantic sector of the Antarctic continent, directly downwind of the South American continent, which is the main dust source for the EAP [e.g., *Delmonte et al*., 2008, *Marino et al*., 2009]. Accordingly, the EDML ice core is excellently suited for high-resolution dust studies during Termination I (hereafter T1). In this paper we present the first dust particle concentration and size record from the Atlantic sector of the EAP covering the time period from 60,000 years B.P. to 7500 years B.P. in subannual resolution and investigate the seasonal phasing of dust concentration and size, which we use as a proxy for the transport intensity. Using a conceptual model, we estimate the effect that a change in seasonality could have on glacial-interglacial dust concentration changes.

2. Methods

Samples for the dust size and concentration analyses were taken using a continuous flow analysis (CFA) melting device, which precluded contact of the melt water with contaminated ice core surfaces [*Kaufmann et al*., 2008; *Röthlisberger et al*., 2000]. Two laser particle detectors (LPD, Abakus, Fa. Klotz, Bad Liebenzell, Germany) were connected to the meltwater flow with a flow rate of 1.6 mL/min. Data were stored every second, yielding subannual resolution records in dust concentration and size covering the Holocene and back to the last glacial. With one LPD only dust concentration was analyzed, whereas with the second LPD dust concentration and size was analyzed. For the dust concentration both detectors revealed the same results. Due to dispersion in the entire melt and dust detector line a nominal depth resolution of approximately 0.5 cm was achieved. The entire EDML ice core starting at a depth of 113 m (~1200 years B.P.) was continuously analyzed down to bedrock. However, below ~2400 m unambiguous dating is not possible; therefore, only results above this depth (corresponding to 145,000 years B.P.) are used here. Some intervals could not be evaluated for high-resolution dust size due to the insufficient core quality in the brittle ice zone interval 700–800 m (14,600–12,000 years B.P.) and in the depth interval 1258–1352 m (35,000–40,000 years B.P.) due to a failure of the LPD. Due to the layer thinning with depth the annual layer thickness below 1710 m was generally below 1.5 cm except for two excursions of thicker layers between 1800 and 1900 m (not shown). Therefore, the dust concentration and size could not be reliably derived in subannual resolution below 1710 m corresponding to ~60,000 years B.P. For the size calibration of the LPD, additional samples were analyzed for dust size and concentration using a Coulter Counter Multisizer II, Beckmann-Coulter (CC). For details of the Multisizer measurements see *Delmonte et al*. [2002]. The calibration method was adopted from *Ruth et al*. [2003]. For each sample measured by CC, the corresponding depth interval measured using the LPD was extracted from the continuous profile. All CC samples were taken from the upper 7 cm of each meter of the core, where the CFA measurement started a new run and often the beginning was affected by contamination or missing ice. If more than 1 cm was missing in the corresponding part of the LPD profile, the sample was not used for the calibration. If in only one of the samples from CC or LPD unusual high concentrations of larger particles were found, this was treated as contamination and the samples were not used for the calibration. Finally, a set of 45 samples was available for the calibration with similar number of Holocene and glacial samples. Beginning with the large particles (to reduce the uncertainty due to noise in the lowermost channels), the number size distribution from the LPD samples was shifted onto the CC spectra for each of the 45 calibration samples. To this end, the bin boundaries of the LPD were adjusted to match the size distributions to the CC results (Figure 1). On the basis of the new bin boundaries a new calibration line was generated for each of the samples. Possible differences in recovery were corrected by the ratio of the concentration measured by both methods. Eventually, the new calibration line was calculated as the mean value of all 45 individual calibration lines. Examples for the Holocene (580 m) and the glacial (1051 m) are given in Figure 1.

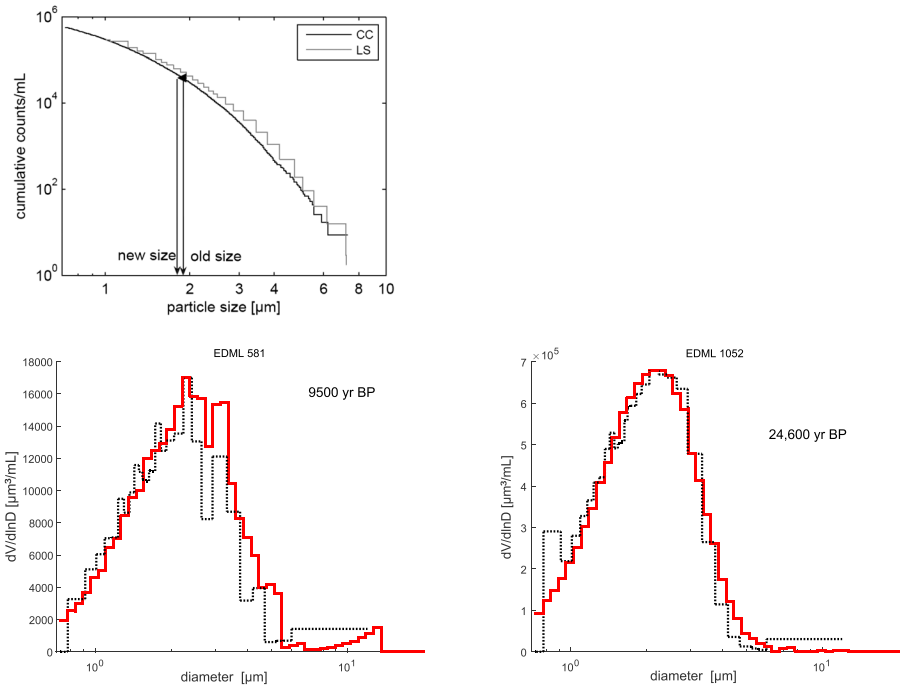

Figure 1. (top) Illustration of the calibration method: The LPD size spectrum (LS) is shifted onto the CC spectrum to obtain new bin sizes. (bottom) Examples for the size distribution used for the calibration from the Holocene (~9500 years B.P., left) and glacial (~24,500 years B.P., right). The LPD data are shown after the adjustment of the size axis and averaging the 45 individual calibration lines. CC data are shown in red; LPD data are shown in black. Note that especially the maximum in the size distribution, which is always at a diameter close to 2 µm, is practically identical for both methods after recalibration.

As a proxy for the dust size, the coarse particle percentage (CPP) was calculated by dividing the volume fraction >2 µm (diameter of a sphere with the same volume as the respective particle) by the total volume concentration (>1 µm). In previous studies the fine particle percentage (FPP volume fraction 1 µm to 2 µm divided by total volume concentration) was widely used [e.g., *Lambert et al.*, 2008], which is the inverse of the CPP. For convenience, we use the CPP, as the value of both CPP and mode increase if more large particles are found in the sample. The uncertainty of the CPP inferred from the counting error of each size bin is usually below 1%. Therefore, we can exclude, that the observed variations are caused by analytical biases. Additionally, for the low-resolution profiles (1 m averages), we used the modal value μ of a fitted logarithmic normal function as a measure for the mean dust size. The uncertainty of the modal value µ is controlled by the counting error of each size bin ($\sqrt{N}$) and the interval chosen for fitting. The influence of the counting statistics was determined by a Monte Carlo technique as follows: 1000 size spectra were calculated, where the counts in each size bin were varied within the counting uncertainty. The mean of the 1000 values for this size bin equaled the measured value $N(r)$ for the specific size bin and the 1σ interval the statistical counting error $\sqrt{N(r)}$ for this size bin with mean radius r. This was done for all size bins yielding 1000 size spectra. The mode obtained by performing a lognormal fit on all those spectra varied within 1σ of less than 0.02 µm for the glacial samples and 0.05 µm for interglacial samples. The influence of the interval chosen for fitting (approximately from 1 to 4 µm) was determined by changing the fitting interval. The range for reasonable values for µ by changing the range of the fitting interval was 0.05 µm for glacial and interglacial values and thus the dominant error compared to the counting error. For the high-resolution dust size measurements, the total number of counted dust particles was often too low to fit a logarithmic normal function and the CPP provided a more robust estimate of changes in dust size. The two different size parameters are interchangeable especially during the glacial and the first part of the transition (Figures 2 and 3). Thus, the use of either of them will not affect the results and the discussion. For the Holocene the CPP appeared to be the more robust parameter. Below 2050 m (corresponding to about 87,000 years B.P.) millimeter-scale z folds and up to 15° tilts start to show up in visible layers in the ice core [*Faria et al.*, 2010]. At that depth CPP and mode start

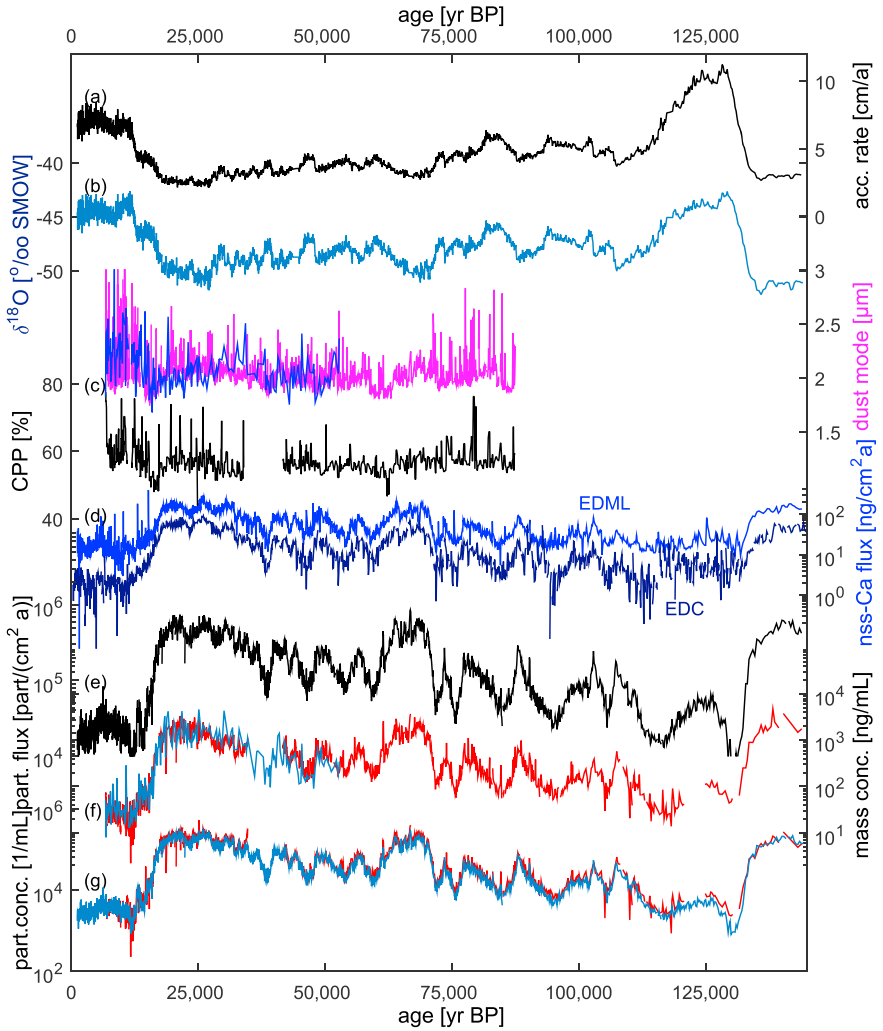

Figure 2. Overview over the EDML dust record: (a) accumulation rates derived from $\delta^{18}O$ [*EPICA-community members*, 2006], (b) $\delta^{18}O$ *EPICA-community members*, 2006], (c) dust size in terms of coarse particle percentage (CPP, ratio of mass of particles larger than 2 µm with respect to total mass, black), modal value of the volume distribution derived from measurements using the LPD (magenta) and CC (blue) (all this study), (d) nss-Ca flux from EDML (light blue) and EDC (dark blue, both [*Kaufmann et al.*, 2010]), (e) dust particle flux (this study), (f) dust mass concentration (this study), and (g) dust particle concentration (this study).

to diverge. Thus, we assume that dust size cannot be reliably reproduced with our methods in this depth interval and the size data are not used here. The concentration does not seem to be affected as shown by the very good correspondence of Ca^{2+} and dust concentration profiles (Figure 2). In the following we will always refer to the CPP. The age scale of the EDML ice core was adopted from AICC2012 [*Veres et al.*, 2013]. For the depth intervals 450–800 m and 1450–1500 m individual layer counting was conducted. For all other depth intervals the AICC2012 age scale was linearly interpolated on 1 m intervals.

3. Results

An overview over the dust concentration, flux, and size in the EDML ice core is shown in Figure 2. Additionally, accumulation rates [*EPICA-community members*, 2006], $\delta^{18}O$ values [*EPICA-community members*, 2006] as an indicator for temperature, and non-sea-salt (nss)-Ca^{2+} fluxes for EDML and EDC quantified using CFA [*Kaufmann et al.*, 2010] as a proxy for the soluble dust fraction are given. Here the dust particle number and dust mass concentrations are given. Mass concentration and number concentration profiles show a very high coherence (Figures 2f and 2g). Further on, only dust mass concentrations will be used (which can be

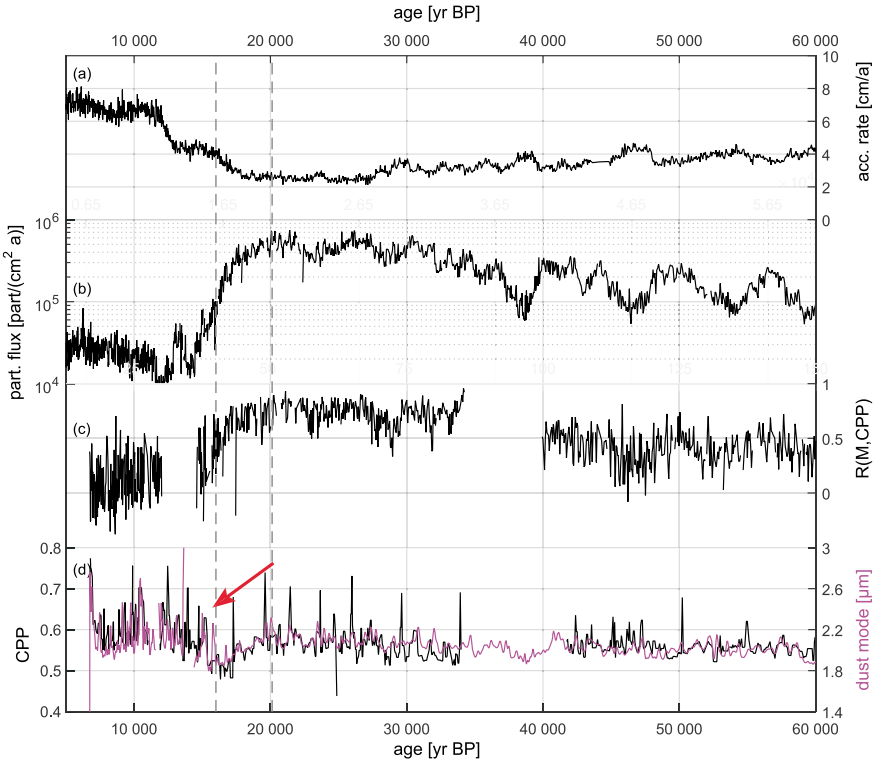

Figure 3. Overview of dust characteristics in EDML during Transition I: (a) accumulation rates derived from $\delta^{18}O$ [*EPICA-community members*, 2006], (b) dust particle flux, (c) correlation coefficient between dust mass and dust size, and (d) dust size in terms of CPP (black) and dust mode (magenta). The red arrow indicates the decrease in dust size between 20,000 years B.P. and 16,000 years B.P. before the dust size increases again at 16,000 years B.P.

directly compared to other geochemically important dust tracers such as Ca^{2+}) and denoted as dust concentration. The complete undisturbed ice core record reaches back to 145,000 years B.P. Below that, unambiguous dating is not possible at the present stage. Down to 60,000 years the annual layer thickness is above 1.5 cm, the limit for the identification of a seasonal signal. Below 1.5 cm, dispersion in the CFA system does not allow to distinguish single years. Accordingly, we will interpret seasonal cycles in dust concentration and size only for the last 60,000 years in this study.

Clearly identifiable are the strongly elevated dust levels during the glacial stage. The mean glacial dust concentration is 46 times higher than during the interglacials (Holocene 7000 years B.P.–10,000 years B.P.: 16–112 ng/mL, glacial 18,000 years B.P.–26,000 years B.P.: 850–4600 ng/mL). However, the absolute minimum of 6 ng/mL in the dust concentration record is reached at ~11,600 years B.P. This is in line with dust concentration ratios of other Antarctic ice cores like Vostok and EPICA Dome C [*Lambert et al.*, 2008; *Petit et al.*, 1999]. In the very low accumulation areas of the high EAP dry deposition of dust aerosol prevails. In this case variations in the dust flux are more representative of accompanying changes in the atmospheric aerosol concentration [*Fischer et al.*, 2007b]. The absolute dust flux in the EDML ice core is about twice as high as at EPICA Dome C due to the closer proximity of the EDML drill site to Southern South America (Figure 2d), the main glacial dust source for the entire EAP and also the predominant Holocene source in the case of EDML [*Wegner et al.*, 2012]. The glacial dust flux at EDML is a factor of 18 higher than in the Holocene. The profiles of the dust concentration and the nss-Ca^{2+} concentration show very good correspondence especially for the parts of the records with higher dust concentrations, where the Ca^{2+} concentration is dominated by input of crustal material.

The dust particle size (given as modal value μ or CPP in Figures 2c and 3d) is slightly larger during the Holocene than during the glacial. However, early during T1, the particle size intermittently decreases even further until about 16,000 years B.P., followed by an increase to the Holocene level. This is in line with results from other Antarctic ice cores. In the EPICA Dome C and Komsomolskaya ice cores, larger particles were also

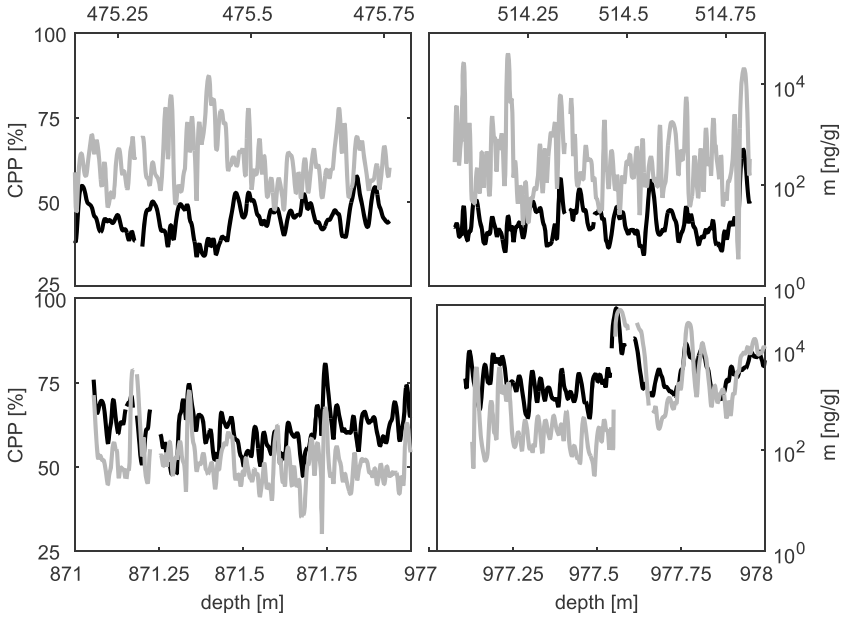

Figure 4. Four examples for size (given in coarse particle percentage CPP, grey) and dust mass concentration (black line) in different climatic stages. Holocene (two upper examples, ~7200 years B.P. and ~8000 years B.P.), transition (lower left ~17,000 years B.P.) and LGM (lower right, ~21,400 years B.P.). The *y* axes are the same in all subfigures. The correlation between concentration and size is higher during the LGM than during the Holocene.

found during warm stages [*Delmonte et al*., 2004]. An evident size minimum during the early deglaciation until 16,000 years B.P. was also observed at Dome C [*Delmonte et al*., 2004] and at Talos Dome [*Albani et al*., 2012a]. For the last glacial, there is no clear correspondence between particle size and temperature or dust concentration. Dust size in the Dome B record shows the opposite glacial/interglacial trend with significantly larger dust particles during the glacial. This has been attributed to regional differences in atmospheric pathways in terms of transport through either advection or subsidence over the EAP [*Delmonte et al*., 2004]. Note that when considering multiannual mean modal values, the results are biased to the modal values occurring during the dust concentration maxima. Thus, a different seasonality in dust concentration and size at different sites may also contribute to the differences in the size record additional to the effect of different atmospheric pathways. It cannot be ruled out, that during different climatic stages, the contribution of particles transported in lower atmospheric levels by advection onto the plateau and particles transported in higher atmospheric levels and subsidence may have changed on seasonal scale. However, due to the lack of seasonally resolved dust size information at other sites, the extent of this effect cannot be quantified at this point.

The high-resolution concentration and size profiles measured in this study allow for the first time also an investigation of the seasonal phase relationship of dust concentration and dust size. Examples for high-resolution size and dust mass concentrations in different climatic stages are given in Figure 4. Here higher covariance of dust concentration and size can be identified during the glacial compared to the Holocene. Figure 5 shows the mean seasonality during a time interval of ~3000 years during the Holocene (6700–9500 years B.P.) and glacial (45,000–48,000 years B.P.). During the glacial, CPP and dust concentration show their maximum approximately during the same time of the year, whereas during the Holocene the maximum of the CPP is opposite to the dust concentration maximum. The lower amplitude during the glacial can be explained by the lower layer thickness and therewith higher dispersion over 1 year. The correlation between the CPP and the dust concentration over 1 m intervals over the past 60,000 is displayed in Figure 3. To investigate the effect of the different time resolution for the Holocene and the glacial, the correlation was also calculated using data on an equidistant timescale in the depth intervals 450–800 m and 1450–1500 m revealing the same results. The high correlation during the glacial ($r = \sim 0.8$) decreases during T1 to very variable and much lower correlation coefficients between 0 and 0.4. Due to bad core quality in the so called "brittle zone," data gaps arise between 12,000 years B.P. and 16,000 years B.P. Additionally,

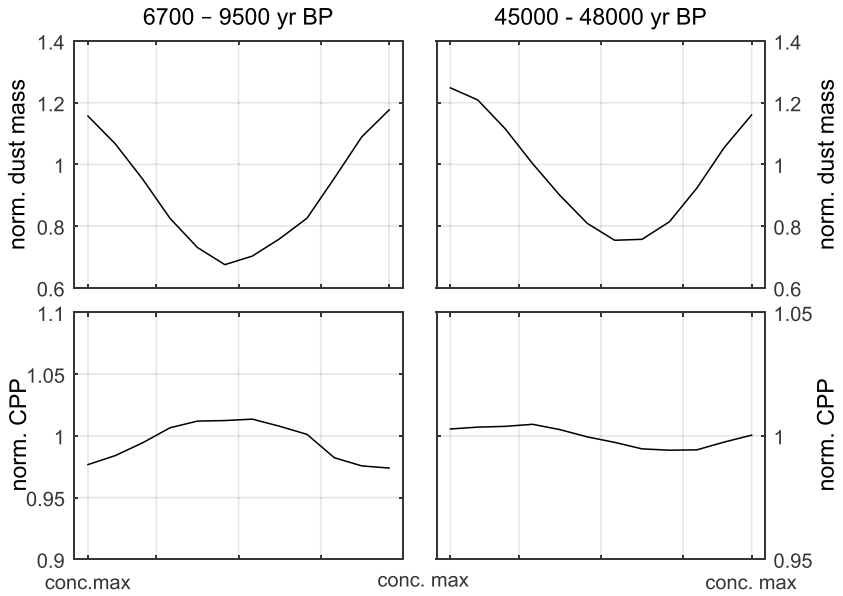

Figure 5. Relative seasonality of (top) dust concentration and (bottom) size (during the Holocene (left) and the glacial (right)): The median of the normalized seasonal cycle of dust mass and concentration was calculated. 12 time steps over 1 year are linear interpolated within one year according to the annual layer counted year based on the ammonium concentration peak. During recent times the dust concentration maximum occurs during winter [*Sommer et al*., 2000]. We assume that the dust concentration maximum also occurs during winter during the time intervals presented here.

between 35,000 years B.P. and 39,000 years B.P., the dust size could not be evaluated in high resolution due to technical failure of the LPD. During Marine Isotope Stage 3 we find lower concentrations in parallel to the major Antarctic isotope maxima (AIM) [*EPICA-community members*, 2006]. The correlation of dust concentration and CPP ranges between $0.2 < r < 0.7$ for these AIM events, with lower correlations during warmer periods.

As mentioned above, a shift in seasonal phasing could have an influence on the multiannual mean values. During warmer climatic stages, we find more often the dust size maximum not to be synchronous with the concentration maximum. The multiannual size mean value is dominated by the size during the dust maximum, thus shifted to larger particles during the glacial compared to the Holocene. The influence of the dust deposited outside the concentration maximum on the multiannual mean size is much smaller. Thus, we conclude, that the increase in size from the glacial to the Holocene cannot be explained by the shift in the seasonal phasing of dust concentration and size.

As mentioned above, the timing of the dust input to Antarctica during the year is not simultaneous at all sites because sources, atmospheric transport dynamics, and processes occurring during transport can be different. To pinpoint the timing during the year when dust input to DML reaches its maximum, the particle and Na^+ concentration profiles during the Holocene were used. At EDML the Na^+ concentration maximum occurs clearly during austral winter [*Sommer et al*., 2000; *Weller and Wagenbach*, 2007]. In order to determine the seasonality of the dust maximum at EDML, first, the maxima in the high-resolution Na^+ concentration profile from the EDML ice core were defined as winter and the distance between adjacent Na^+ concentration maxima were subdivided in 12 equidistant intervals. The position of the dust concentration maximum in one of the 12 intervals was then determined (Figure 6). Note that this plot does not show the mean seasonality but the timing of the dust peak. Dust maxima occur during all times of the year. However, most maxima are found at the same time as the Na^+ concentration maximum during winter with a probability of dust maximum occurrence twice as high as during summer. The analysis technique used to determine Na^+ concentrations causes larger dispersion than the determination of Ca^{2+} and dust concentrations. Thus, the investigation of the phase lag of Na^+ and Ca^{2+} as well as dust concentrations cannot be performed for the deeper part at 1450 m–1500 m, where dust concentrations still show a seasonal signal, whereas seasonal variability in Na^+ concentration is completely smoothed out in the CFA data.

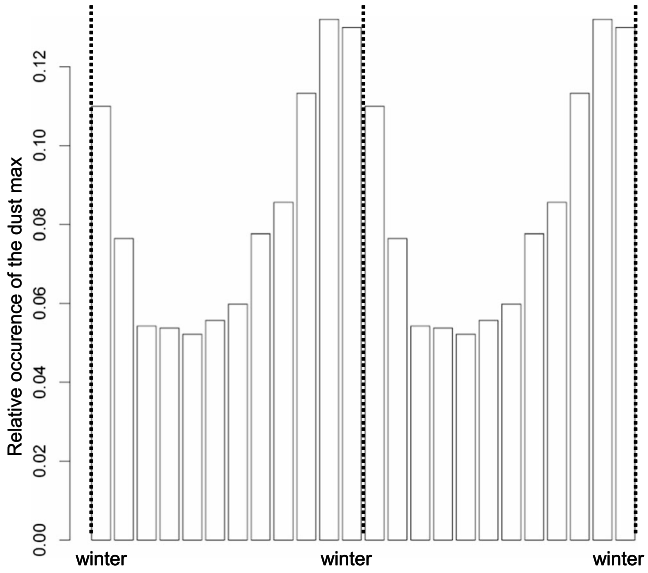

Figure 6. Histogram of the seasonal occurrence of the dust maxima at EDML relative to the Na^+ concentration maximum in winter. The dashed lines indicate the maximum of the Na+ concentration over the Holocene (~2000 years B.P.–~15,000 years B.P.). The dust peak occurs twice as likely in winter than in summer.

4. Discussion

4.1. Multiannual Mean Values

First, we will focus on the multiannual mean values of the dust proxies with emphasis on the dust size. The decrease of the dust concentration during T1 starts around 20,000 years B.P. (Figure 3). Simultaneously, also the dust size starts to decrease until ~16,000 years B.P., where a sharp increase in the dust size to larger Holocene values can clearly be discerned. This intermittent decrease in dust size during T1 could also be observed in Dome C and Talos Dome [*Delmonte et al*., 2004; *Albani et al*., 2012a]. At the same time, the chemical signature of the dust changes in DML and Dome C [*Röthlisberger et al*., 2002; *Gabrielli et al*., 2010; *Wegner et al*., 2012]. A divergence between the dust flux in Talos Dome and Dome C, was found after 16,000 years B.P. with a higher ratio between Talos Dome and EDC dust fluxes after 16,000 years B.P. compared to the time before [*Albani et al*., 2012b]. Summarizing the observations from the Antarctic dust records, evidence increases that around 16,000 years B.P. a significant change occurred in either the sources or the transport characteristics of dust, which had an Antarctic wide influence on the dust deposition.

In previous studies the glacial/interglacial decrease in the dust flux was explained by an increased hydrological cycle, weaker source emissions and a change in atmospheric transport [e.g., *Petit et al*., 1999, *Fischer et al*., 2007b]. *Röthlisberger et al*. [2002] attributes the changes in dust flux during the first part of T1 (until 15,000 years B.P.) mainly to changes in the source areas (vegetation cover and local climate) and the further decrease to a reorganization of atmospheric circulation. From a sediment core offshore Chile at 41°S an increase in sea surface temperatures (SSTs) occurred mainly between 18,800 years B.P. and 16,700 years B.P. [*Lamy et al*., 2007], which is closely linked to the position of the southern westerly wind belt, which has large impacts on the uplift and long range transport of dust from Patagonia, the main source area until 16,000 years B.P. *Stenni et al*. [2010] observed a different climatic evolution between the Atlantic and the Indo-Pacific sector between 16,000 years B.P. and 14,500 years B.P. with a deceleration of the warming in the Atlantic Sector connected to different shifts in moisture sources, which is explained by a reorganization of the atmospheric circulation. Taking these facts together, evidence becomes stronger that T1 can be subdivided into two parts. During the first part from 20,000 years B.P. until around 16,000 years B.P. gradual processes like a weakening of the source due a shift in the westerly wind belt cause the decrease in dust concentration. Around 16,000 years B.P., a more abrupt change happened with an Antarctic wide atmospheric reorganization that allowed more direct transport of dust indicated by larger particles to DML.

The dust size is modulated by changes in transport time and pathways [*Ruth et al*., 2003, *Fischer et al*., 2007b] as well as the snow accumulation rate through atmospheric scavenging processes. The significant warming between 18,000 and 16,000 years B.P. and further on during the transition suggests also an increasing accumulation rate at this time [*EPICA-community members*, 2004, 2006], which would favor smaller particles in the ice at the onset of the termination. This is suggested by the dust size change in Figure 3; however, the change in the accumulation rate, which is significantly less than a factor of 2 at this point, cannot quantitatively explain the accompanying decrease in dust concentration of about a factor of 10. Additionally, the dust size starts to decrease already at 20,000 years B.P. whereas the increase of accumulation rate seem to start slightly later. Thus, especially during the time between 20,000 years and 18,000 years B.P. accumulation rate changes

probably does not account for a reduction in dust size. Alternatively, a less efficient transport at the onset of the termination could contribute to the smaller particles at that time and would also slightly reduce the dust concentration. However, the main driver of the tenfold decrease in dust concentration in this time interval appears to be a reduction in source strength.

After 16,000 years B.P. the dust concentration continues to decrease but the dust size is increasing. This occurs at a time where accumulation rates continue to rise significantly and, thus, we can exclude that accumulation rate accounts for the change in dust size. At that time the transport effect must overcompensate a reduced relative contribution of size-fractionating dry deposition and we conclude that after 16,000 years B.P. transport must have intensified or different transport pathways enabling larger particles to reach DML became more important. This explanation holds both for EDML, for EDC and for Komsomolskaya but cannot explain the opposite glacial/interglacial change of dust size at Dome B. The latter may reflect a regional difference in dust transport [*Delmonte et al*., 2004]. A more efficient transport for dust to the EAP during the second part of the transition, however, would also lead to higher dust concentrations. This may be partly compensated by the stronger wash out of particles en route reducing the atmospheric life time of dust and the higher snow accumulation at that time leading to a dilution of dust concentrations in the ice. Also, a decrease in the source strength occurring simultaneously could lead to a decreased dust concentration in the ice. If the accompanying change in Rare Earth element composition at ~16,000 years B.P. [*Wegner et al*., 2012] is due to a strong reduction of one source, this supports the latter explanation. The total change in dust concentration after 16,000 years B.P. to the Holocene is a decline by a factor of 4–5, which is in the possible range of the combined effects on dust concentration by stronger wet deposition during transport and at the ice core drill sites (see also section on seasonality below). Interestingly, such competing effects of shortened transport time and significantly reduced atmospheric lifetime are in general agreement with little net change in the difference between dust fluxes between EDML and EDC over time [*Fischer et al*., 2007a], assuming a major Patagonian dust contribution for both sites. Note, however, that for sites in the Indo-Pacific sector of the EAP such as Dome C other sources than Patagonia become relatively more important in the late stage of the transition.

Thus, we conclude that during the first part of T1 up to 16,000 years B.P., where only South American dust is identified in East Antarctica, a reduced emissivity of the source must have occurred accompanied by a less effective transport. Additionally, an increase of wet deposition could have played a minor role. After 16,000 years B.P. the source strength may have continued to decline but a reorganization of atmospheric circulation allowed for faster dust transport or different transport pathways but significantly increased wash out of dust during transport.

4.2. High-Resolution Dust Concentration and Size Profile

Quantitatively disentangling the contribution of different processes to the large glacial/interglacial variability in dust concentration in ice cores is a key question. Here we propose a new approach using subannual resolution dust concentration and size profiles to investigate possible seasonal processes contributing to the decrease in dust flux over T1.

The main processes influencing the dust concentration in the snow C_{snow} for different time periods ($t1$ and $t2$) are the source emission strength E, the transport efficiency T, and processes related to the deposition D with

$$\frac{C_{t1}}{C_{t2}} = \frac{E_{t1}}{E_{t2}} \cdot \frac{T_{t1}}{T_{t2}} \cdot \frac{D_{t1}}{D_{t2}} \quad (1)$$

Martínez-Garcia et al. [2009] found a factor of 5 higher dust fluxes in the glacials compared to interglacials in a sediment core from the South Atlantic, at a site directly downwind Patagonia, the main dust source for the EAP during glacials [e.g., *Delmonte et al*., 2008; *Marino et al*., 2009; *Gabrielli et al*., 2010] and for DML also during the Holocene [*Wegner et al*., 2012]. Thus, this record can be taken as an estimate for the ratio in the Patagonian dust source emission strength between the last glacial and the Holocene. *Petit and Delmonte* [2009] derived a factor of 2–4 change in apparent source strength slightly lower than *Martínez-Garcia et al*. [2009]. Since on the EAP most of the dust is deposited by dry deposition, the increase in snow accumulation between the last glacial to the Holocene accounts for another factor of 2 in the dust concentration [*EPICA-community members*, 2006]. Overall changes in emission strength together with changes in local

deposition over the ice sheet (due to the lower glacial accumulation rate) can explain about a factor of 10 (out of 46) in the glacial/interglacial dust concentration change. Accordingly, another factor of 4–5 is missing in the budget.

As outlined above the increase in dust size in the later part of the transition implies a faster or more direct transport and thus a tendency to higher concentration at that time, which is the opposite to the observed decrease in dust concentration during that time. When looking at multiannual mean modal values, the obtained size is biased to the sizes occurring during the dust concentration maxima, which could affect the estimates for the glacial/interglacial change in dust concentration. In this study, we address the question how much of the glacial-interglacial dust concentration changes can be attributed to a change in the seasonal phasing of dust transport and dust emission. Needless to say that other processes such as a reduced hydrological cycle and the larger amount of total emitted dust during the glacial are other important factors influencing the dust concentration in Antarctic ice cores.

To explain the effect of the phase lag in dust concentration and size on the glacial/interglacial dust difference, we apply a simple conceptual model for the dust transport from the dust source to the ice sheet.

Taking into account a seasonal variability in each of the components equation (1) turns into

$$C_{\mathrm{snow}}(t) = E(t)\cdot T(t)\cdot D(t) \tag{2}$$

where t is the time of the year. The maximum of the dust storm frequency in Patagonia at present day occurs in summer [*Johnson et al.*, 2010]. This already shows that the occurrence of the dust maximum in EDML in winter for interglacial conditions cannot be explained by the emission seasonality $E(t)$, but is controlled by the recent seasonality in transport and/or deposition.

To estimate a magnitude of the effect of seasonality with our simple model approach, we describe the dust emission $E(t)$ with a sin function

$$E(t) = \Delta E \cdot \sin(\omega_E \cdot t) + \overline{E} \tag{3}$$

with $\bar{E}$ the mean total emission flux per year, $\omega_E = 2\pi/(1\ \mathrm{year})$ and t given in years. ΔE accounts for the seasonal amplitude in source, with $\Delta E < \bar{E}$, to exclude a negative value for the source strength.

Based on an atmospheric model, the simulated tracer age [*Krinner and Genthon*, 2003] at the EDML drill site as a proxy for the age of the air mass reaching the site is smaller in austral winter than summer for present day and the Last Glacial Maximum (LGM). However, the absolute modeled tracer age is smaller in the LGM compared to present day. Also, backtrajectory studies [*Reijmer et al.*, 2002] show a clear seasonal cycle in transport times of air masses reaching the EAP. In this meteorological study recent transport to EDML is also slowest in austral summer and more efficient in winter but most efficient in austral spring. In any case a significant seasonal variation in transport time for dust transport to EDML can be expected. We describe the transport with a sine function

$$T(t) = \Delta T \cdot \sin(\omega_T \cdot t + \varphi) + \overline{T} \tag{4}$$

With $\overline{T}$ the mean transport intensity during 1 year, $\omega_T = 2\pi/1$ year and $0 < \varphi < 2\pi$. ΔT accounts for the seasonal amplitude in transport efficiency, with $\Delta T < \overline{T}$, to exclude transport from Antarctica to the source area. The phase $0 < \varphi < 2\pi$ accounts for the case that dust emission and transport occurs at different times of the year.

Wet deposition of dust particles occurs in combination with snow accumulation, whereas dry dust deposition is caused by gravitational fallout. At present day about 75% of the dust is estimated to be dry deposited at DML [*Fischer et al.*, 2007b]. During the glacial, when accumulation rates in DML were similar to present-day Dome C accumulation, almost all dust is expected to be dry deposited [*Fischer et al.* 2007b]. The overall higher snow accumulation during the Holocene shifts the modal value of the dust volume distribution to smaller values during wet deposition but does not change the seasonality in dust deposition per se. Here the seasonal variation in snow accumulation and its glacial/interglacial change have to be considered. For instance a higher snow accumulation in winter as suggested by *Laepple et al.* [2011] will favor smaller particles to be deposited during that season. Dependent on the seasonality of dust transport, the seasonal preference of larger dust particles due to changes in the transport time may be either compensated or amplified by the seasonality in precipitation. For present day there exist no reliable seasonally resolved precipitation measurements for the EDML drill site. For other sites on the EAP higher snow accumulation rates were estimated for

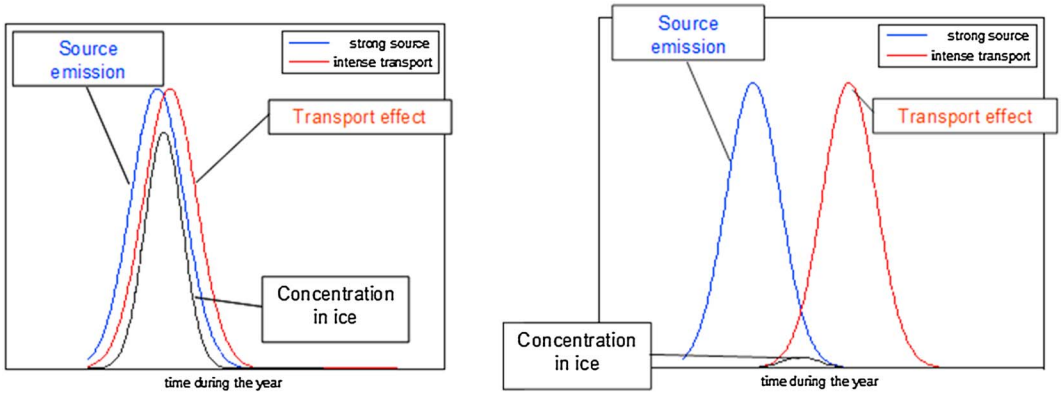

Figure 7. Illustration of the conceptual model for the phasing of dust transport and source emission strength. (left) Maximum dust emission and maximum transport intensity occur simultaneously during the year (left) as is the case during glacial conditions. (right) A phase shift between the two effects results in a significantly lower dust concentration in the ice.

austral winter [*Laepple et al.*, 2011, and references therein]. The snow height recorded by an automatic weather station in the vicinity of the EDML drill site does not provide a picture representative of the seasonality in precipitation [*Welker et al.*, 2015], but modeling studies suggest that most precipitation is supplied by single snowfall events distributed randomly over the year [*Reijmer and van den Broeke*, 2001; *Schlosser et al.*, 2010]. For the last glacial there exists no direct estimates of the seasonality in precipitation at all for Antarctica; however, there is no indication for a changed seasonality compared to present day [*Laepple et al.*, 2011]. To assess the effect of seasonality on the change in the glacial/interglacial dust budget, only the change in precipitation seasonality between glacial and Holocene has to be considered. Here we assume that the seasonality in precipitation [*Laepple et al.*, 2011] and thus $D(t)$ has not changed over time. Accordingly, in the following we will neglect the influence of changes in deposition seasonality in our model.

By using equations (2)–(4) with variable φ, we can describe a variable phase lag between dust emission and dust transport intensity throughout the year (illustrated in Figure 7). For variable φ and fixed ΔT, ΔE, $\overline{T}$, and $\bar{E}$ we calculated the correlation coefficient r between T and C_{snow}.

In the following we estimate how the phase lag between T and C influences the loss compared to in-phase emission and transport. Note, however, that the results still depend on the values of $\bar{E}$, $\overline{T}$, and ΔE, ΔT in equations (3) and (4). Figure 8 illustrates the reduction of the dust concentration between source and sink solely from a changed phase lag of dust emission and transport. For aligned maxima of $E(t)$ and $T(t)$ ($\varphi = 0$) the reduction is 1. With increasing φ the loss due to the changed phase lag increases to a minimum at $\varphi = \pi$. This implies that for an out-of-phase relationship between emission and transport efficiency the high dust load at the source cannot by efficiently transported to Antarctica.

For the last glacial maximum we find correlation coefficients $r(\mathrm{CPP,C}) \sim 0.8$ between the dust size and concentration. Taking this as an estimate for $r(T,C)$, the corresponding value $(\mathrm{E}\cdot\mathrm{T})_{\mathrm{norm}} = (\mathrm{E}\cdot\mathrm{T}(\varphi))/(\mathrm{E}\cdot\mathrm{T}(\varphi = 0))$ ranges between $0.8 < (E\cdot T)_{\mathrm{norm}} < 0.85$ dependent on $\overline{T}/\Delta T$ corresponding to a reduction of the maximum possible $(E\cdot T)_{\mathrm{norm}}$ to ~ 80–85% (indicated as horizontal and vertical dashed lines in Figure 9). For typical Holocene correlation coefficients $0 < r(T,C) < 0.4$, the corresponding value of $(E\cdot T)_{\mathrm{norm}}$ ranges between $0.32 < (E\cdot T)_{\mathrm{norm}} < 0.68$ dependent on $\overline{T}/\Delta T$. With our conceptual model approach this corresponds to a reduction of $(E\cdot T)_{\mathrm{norm}}$ to ~32–50%, i.e., a factor of 2 reduction of $(E\cdot T)_{\mathrm{norm}}$ relative to its glacial value solely due to the dephasing of emission and transport seasonality. Note that the higher the background transport intensity given by $\overline{T}$ the smaller is the influence of the seasonality. For $\overline{T}/\Delta T = 1$, $(E\cdot T)_{\mathrm{norm}}$ is reduced by approximately a factor of 2 from ~0.8 to 0.32–0.5. However, for $\overline{T}/\Delta T = 1.5$, $(E\cdot T)_{\mathrm{norm}}$ is reduced by a factor of 1.4 from ~0.85 to 0.55–0.65 between the glacial and the Holocene.

As $(E\cdot T)_{\mathrm{norm}}$ gives the contribution of a change in the seasonality to the observed glacial/interglacial dust decrease, in this simple model approach we find a possible influence of a changed seasonality between dust concentration and size of a factor of 1.5–2 contributing to the glacial/interglacial dust concentration in EDML

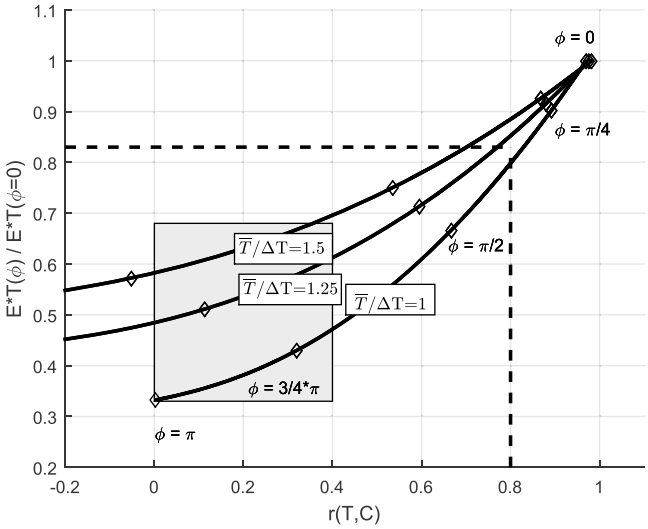

Figure 8. Product of transport efficiency T and source emission strength E ($E \cdot T(\varphi)$)/($E \cdot T(\varphi = 0)$) versus correlation coefficient r between dust concentration in the ice core C and transport intensity T for different φ and different $\overline{T}/\Delta T$ (equation (4)). This figure illustrates the reduction of dust in the ice due to a phase shift between maximum transport efficiency and the maximum of source emission strength. The dashed lines illustrate the mean correlation coefficient of CPP and dust concentration during the glacial. The grey square gives the range of respective correlation coefficients during the Holocene.

change dependent on the phasing of $E(t)$ and $T(t)$. The maximum effect is achieved if emission and transport where in-phase during the glacial and uncorrelated in the interglacial, as suggested by our high-resolution dust data.

What causes the dephasing of emission and transport during the transition? A contribution by other dust sources like Australia during a different season could influence our estimate. At present day, the highest frequency of dust storms in Australia occurs in spring to summer [*Ekström et al*., 2004], exhibiting only a small shift compared to the summer maximum in Southern South America. As the dust input to DML is dominated by South American dust, the minor contribution by Australian dust is not expected to change the seasonal signal in the dust record significantly. Alternatively, local sources in the Transantarctic Mountains could act as a dust supplier but mainly for larger particles. Another possible contribution to the dust input to DML could originate from the Puna Altiplano (PAP) in Bolivia. There is no study yet, that could distinguish from where in South America the dust reaching DML originates from. In the PAP most of the annual precipitation occurs during austral summer. The maximum wind speed is observed during winter and early spring, when the subtropical jet stream crosses the PAP [*Clapperton*, 1993]. In contrast to dust emission from Southern Patagonia, this favors the dust emission in austral winter and early spring. Studies on Sr and Nd isotopes indicate that the PAP has contributed to the dust input in the Indian sector of the East Antarctic plateau as a second contributor besides the Patagonian Pampa [*Gaiero*, 2007; *Delmonte et al*., 2008]. The proximity to DML makes it likely, that the PAP might have contributed to the dust input in DML. Thus, additional to the summer emissions from Patagonia a contribution from the PAP during winter and early spring, when dust transport intensity is strongest [*Krinner and Genthon*, 2003] or a contribution from local sources cannot be ruled out and could lead to a decorrelation of dust concentration and size. To further evaluate the possibility, if different dust sources contribute during different times of the year, provenance studies in seasonal resolution as the one performed by *Bory et al*. [2010] in Berkner Island are needed.

In summary we can draw the following picture of the main factors influencing the dust reaching DML during the glacial and the Holocene: During the glacial a longer atmospheric lifetime and stronger dust emissions lead to more dust in the atmosphere especially over the sources. Under favorable glacial conditions for intensified direct transport (indicated by larger particles) a synchronous seasonal maximum occurs in DML in dust size and concentration. During the Holocene a shorter atmospheric lifetime and a weaker source lead to a general reduction of the amount of dust in the atmosphere over the source. However, during the Holocene, favorable conditions for intensified transport (indicated by larger particles) are mostly seasonally decoupled from elevated concentrations at the source and thus no dust concentration maximum occurs in DML at the same time.

A stronger coupling between the Antarctic climate and the southern hemisphere midlatitude climate during glacial times compared to warm stages was already proposed by *Lambert et al*. [2008]. A high atmospheric dust concentration over the source during favorable transport conditions leads to a more direct transfer of the climatic signal from South America to Antarctica, resulting in a stronger coupling of the two regions supporting the results by *Lambert et al*. [2008]. The onset of the major deglacial decrease in dust concentration occurs simultaneously with the increase in temperature (expressed as $\delta^{18}O$ values, Figure 3) and the decrease of the correlation between dust concentration and size around 20,000 years B.P. (Figure 6). This coincides with the southward displacement of the westerly wind belt [*Lamy et al*., 1999], indicating that the westerly wind belt may have played a major role for the emission strength of the dust sources in Southern South America. In this respect the long-term changes in dust size distribution at EDML may be also partly interpreted to reflect changes in the position of the westerly wind belt.

5. Conclusions

In this study we investigated for the first time the dust concentration and size in the Atlantic sector of the EAP and its seasonal phasing over the last 60,000 years B.P. We find 46 times higher dust concentrations and smaller dust particles during the LGM compared to the Holocene. In the interval 20,000–16,000 years B.P. a reduced emissivity of the source area compared to the peak glacial and a reduction in transport intensity are identified as the main factors controlling the dust concentration decrease in Antarctic ice cores. An abrupt increase in dust size and a change in the dust provenance indicate an atmospheric reorganization at around 16,000 years B.P. Adding to previously proposed interpretations, where differences in dust sizes were explained by transport in different atmospheric altitudes [*Delmonte et al*., 2004, 2005], we propose an additional effect acting on seasonal scale at EDML. We find a high correlation of $r = 0.8$ between dust size and dust concentration in the ice during the cold glacial and lower values with higher variability during warmer stages with $0 < r < 0.4$ during the Holocene. We argue that dust input to Dronning Maud Land is much more efficient if dust emission and favorable dust transport conditions occur at the same time of the year. According to our study at EDML, this is the case during colder climate and but not during warmer climate. Applying a conceptual model approach using the dust size as a proxy for transport we derive a contribution of a factor of 1.5–2 to the observed factor of 46 of the glacial-interglacial dust concentration decrease at EDML by decoupled changes in seasonality of dust emission and transport. Together with the glacial/interglacial source change estimate derived from marine records in the Atlantic sector of the Southern Ocean [*Martínez-Garcia et al*., 2009] of a factor of 5 and a doubling of the accumulation rate from glacial to interglacial conditions (changing the total dust deposition at the drill site) this leaves a further reduction factor of 2–3 to be explained by the net change in atmospheric aerosol concentrations due to transport effects like increased washout en route, where a shorter lifetime during warm conditions overcompensates the somewhat faster transport.

Acknowledgments

We thank two anonymous reviewers for useful suggestions to improve the manuscript. This work is a contribution to the European Project for Ice Coring in Antarctica (EPICA), a joint European Science Foundation/European Commission Scientific Programme, funded by the EU and by national contributions from Belgium, Denmark, France, Germany, Italy, the Netherlands, Norway, Sweden, Switzerland, and the United Kingdom. The main logistic support was provided by IPEV and PNRA (at Dome C) and AWI (at Dronning Maud Land). This is EPICA publication no. 301. The Division for Climate and Environmental Physics, Physics Institute, University of Bern acknowledges the long-term financial support of our Continuous Flow Analysis on ice cores by the Swiss National Science Foundation (SNSF). Anna Wegner thanks DGF and REKLIM for funding. Data are available on www.pangaea.de.

References

Albani, S., B. Delmonte, V. Maggi, C. Baroni, J.-R. Petit, B. Stenni, C. Mazzola, and M. Frezzotti (2012a), Interpreting last glacial to Holocene dust changes at Talos Dome (East Antarctica): Implications for atmospheric variations from regional to hemispheric scales, *Clim. Past*, *8*, 741–750, doi:10.5194/cp-8-741-2012.

Albani, S., N. M. Mahowald, B. Delmonte, V. Maggi, and G. Winckler (2012b), Comparing modeled and observed changes in mineral dust transport and deposition to Antarctica between the Last Glacial Maximum and current climates, *Clim. Dyn.*, doi:10.1007/s00382-011-1139-5.

Bory, A., E. Wolff, R. Mulvaney, E. Jagoutz, A. Wegner, U. Ruth, and H. Elderfield (2010), Multiple sources supply eolian mineral dust to the Atlantic sector of coastal Antarctica: Evidence from recent snow layers at the top of Berkner Island ice sheet, *Earth Planet. Sci. Lett.*, *291*, 138–148, doi:10.1016/j.epsl.2010.01.006.

Burn-Nunes, L., et al. (2011), Seasonal variability in the input of lead, barium and indium to Law Dome Antarctica, *Geochim. Cosmochim. Acta*, *75*, 1–20, doi:10.1016/j.gca.2010.09.037.

Clapperton, C. (1993), *Quaternary Geology and Geomorphology of South America*, 780 pp., Elsevier, Amsterdam.

Delmonte, B., J. R. Petit, and V. Maggi (2002), Glacial to Holocene implications of the new 27000-year dust record from the EPICA Dome C (East Antarctica) ice core, *Clim. Dyn.*, *18*, 647–660, doi:10.1007/s00382-001-0193-9.

Delmonte, B., J. R. Petit, K. K. Andersen, I. Basile-Doelseh, V. Maggi, and V. Y. Lipenkov (2004), Dust size evidence for opposite regional atmospheric circulation changes over east Antarctica during the last climatic transition, *Clim. Dyn.*, *23*, 427–438, doi:10.1007/s00382-004-0450-9.

Delmonte, B., J. R. Petit, G. Krinner, V. Maggi, J. Jouzel, and R. Udisti (2005), Ice core evidence for secular variability and 200-year dipolar oscillations in atmospheric circulation over East Antarctica during the Holocene, *Clim. Dyn.*, *24*, 641–654, doi:10.1007/s00382-005-0012-9.

Delmonte, B., P. S. Andersson, M. Hansson, H. Schoeberg, J. Petit, I. Basile-Doelsch, and V. Maggi (2008), Aeolian dust in East Antarctica (EPICA-Dome C and Vostok): Provenance during glacial ages over the last 800 kyr, *Geophys. Res. Lett.*, *35*, L07703, doi:10.1029/2008GL033382.

Delmonte, B., P. S. Andersson, H. Schöberg, M. Hansson, J. R. Petit, R. Delmas, D. M. Gaiero, V. Maggi, and M. Frezzotti (2010), Geographic provenance of aeolian dust in East Antarctica during Pleistocene glaciations: Preliminary results from Talos Dome and comparison with East Antarctic and new Andean ice core data, *Quat. Sci. Rev.*, *29*(1–2), 256–264, doi:10.1016/j.quascirev.2009.05.010.

Ekström, M., G. H. McTainsh, and A. Chappell (2004), Australian dust storms: Temporal trends and relationships with synoptic pressure distributions (1960–99), *Int. J. Climatol.*, *24*(12), 1581–1599, doi:10.1002/joc.1072.
EPICA-Community Members (2004), Eight glacial cycles from an Antarctic ice core, *Nature*, *429*, 623–628, doi:10.1038/nature02599.
EPICA-Community Members (2006), One-to-one coupling of glacial climate variability in Greenland and Antarctica, *Nature*, *444*, 195–198, doi:10.1038/nature05301.
Faria, S., J. Freitag, and S. Kipfstuhl (2010), Polar ice structure and the integrity of ice-core paleoclimate records, *Quat. Sci. Rev.*, *29*, 338–351, doi:10.1016/j.quascirev.2009.10.016.
Fischer, H., et al. (2007a), Reconstruction of millenial changes in the dust emission, transport and regional sea ice coverage using the deep EPICA ice cores from the Atlantic and the Indian sector of Antarctica, *Earth Planet. Sci. Lett.*, *260*, 340–354, doi:10.1016/j.epsl.2007.06.014.
Fischer, H., M. L. Siggaard-Andersen, U. Ruth, R. Röthlisberger, and E. Wolff (2007b), Glacial/interglacial changes in mineral dust and sea-salt records in polar ice cores: Sources, transport, and deposition, *Rev. Geophys.*, *45*, RG1002, doi:10.1029/2005RG000192.
Gabrielli, P., et al. (2010), A major glacial-interglacial change in aeolian dust composition inferred from Rare Earth Elements in Antarctic ice, *Quat. Sci. Rev.*, *29*, 265–273, doi:10.1016/j.quascirev.2009.09.002.
Gaiero, D. M. (2007), Dust provenance in Antarctic ice during glacial periods: From where in southern South America?, *Geophys. Res. Lett.*, *34*, L17707, doi:10.1029/2007GL030520.
Gasso, S., A. Stein, F. Marino, E. Castellano, R. Udisti, and J. Ceratto (2010), A combined observational and modeling approach to study modern dust transport from the Patagonia desert to East Antarctica, *Atmos. Chem. Phys.*, *10*, 8287–8303, doi:10.5194/acp-10-8287-2010.
Johnson, M., N. Meskhidze, F. Solmon, S. Gassó, P. Chuang, D. Gaiero, R. Yantosca, S. Wu, Y. Wang, and C. Carouge (2010), Modeling dust and soluble iron deposition to the South Atlantic Ocean, *J. Geophys. Res.*, *115*, D15202, doi:10.1029/2009JD013311.
Kaufmann, P., U. Federer, M. A. Hutterli, M. Bigler, S. Schüpbach, U. Ruth, J. Schmitt, and T. F. Stocker (2008), An improved Continuous Flow Analysis (CFA) system for high-resolution field measurements on ice cores, *Environ. Sci. Technol.*, *42*, 8044–8050, doi:10.1021/es8007722.
Kaufmann, P., et al. (2010), Ammonium and non-sea salt sulfate in the EPICA ice cores as indicator of biological activity in the Southern Ocean, *Quat. Sci. Rev.*, *29*, 313–323, doi:10.1016/j.quascirev.2009.11.009.
Kok, J. (2011), Does the size distribution of mineral dust aerosols depend on the wind speed at emission?, *Atmos. Chem. Phys.*, *11*, 10,149–10,156, doi:10.5194/acp-11-10149-2011.
Krinner, G., and C. Genthon (2003), Tropospheric trana under varying climatic conditions, *Tellus*, *55B*, 54–70.
Laepple, T., M. Werner, and G. Lohmann (2011), Synchronicity of Antarctic temperatures and local solar insolation on orbital timescales, *Nature*, *471*, 91–94, doi:10.1038/nature09825.
Lambert, F., B. Delmonte, J. R. Petit, M. Bigler, P. R. Kaufmann, M. A. Hutterli, T. F. Stocker, U. Ruth, J. P. Steffensen, and V. Maggi (2008), Dust-climate couplings over the past 800,000 years from the EPICA Dome C ice core, *Nature*, *452*, 616–619, doi:10.1038/nature06763.
Lambert, F., M. Bigler, J. P. Steffensen, M. Hutterli, and H. Fischer (2012), Centennial mineral dust variability in high-resolution ice core data from Dome C, Antarctica, *Clim. Past*, *8*, 609–623, doi:10.5194/cp-8-609-2012.
Lamy, F., D. Hebbeln, and G. Wefer (1999), High-Resolution Marine Record of Climatic Change in Mid-latitude Chile during the Last 28,000 Years Based on Terrigenous Sediment Parameters, *Quat. Res.*, *51*, 83–93, doi:10.1006/qres.1998.2010.
Lamy, F., J. Kaiser, H. W. Arz, D. Dierk Hebbeln, U. Ninnemann, O. Timm, A. Timmermann, and J. R. Toggweiler (2007), Modulation of the bipolar seesaw in the Southeast Pacific during Termination 1, *Earth Planet. Sci. Lett.*, *259*, 400–413, doi:10.1016/j.epsl.2007.04.040.
Mahowald, N. M., and L. M. Kiehl (2003), Mineral aerosol and cloud interactions, *Geophys. Res. Lett.*, *30*(9), 1475, doi:10.1029/2002GL016762.
Mahowald, N., S. Albani, S. Engelstaedter, G. Winckler, and M. Goman (2011), Model insight into glacialeinterglacial paleodust records, *Quat. Sci. Rev.*, *30*, 832–854, doi:10.1016/j.quascirev.2010.09.007.
Marino, F., E. Castellano, S. Nava, M. Chiari, U. Ruth, A. Wegner, F. Lucarelli, R. Udisti, B. Delmonte, and V. Maggi (2009), Coherent composition of glacial dust on opposite sides of the East Antarctic Plateau inferred from the deep EPICA ice cores, *Geophys. Res. Lett.*, *36*, L23703, doi:10.1029/2009GL040732.
Martínez-Garcia, A., A. Rosell-Melé, W. Geibert, R. Gersonde, P. Masqué, V. Gaspari, and C. Barbante (2009), Links between iron supply, marine productivity, sea surface temperature, and CO_2 over the last 1.1 Ma, *Paleoceanography*, *24*, PA1207, doi:10.1029/2008PA001657.
McConnell, J. R., A. J. Aristarain, J. R. Banta, P. R. Edwards, and J. C. Simoes (2007), 20th-Century doubling in dust archived in an Antarctic Peninsula ice core parallels climate change and desertification in South America, *Proc. Natl. Acad. Sci. U.S.A.*, *104*(14), 5743–5748, doi:10.1073/pnas.0607657104.
Petit, J. R., and B. Delmonte (2009), A model for large glacial–interglacial climate-induced changes in dust and sea salt concentrations in deep ice cores (central Antarctica): Palaeoclimatic implications and prospects for refining ice core chronologies, *Tellus*, *61B*, 768–790, doi:10.1111/j.1600-0889.2009.00437.x.
Petit, J. R., et al. (1999), Climate and atmospheric history of the past 420 000 years from the Vostok ice core, Antarctica, *Nature*, *399*, 429–436, doi:10.1038/20859.
Reijmer, C. H., and M. R. van den Broeke (2001), Moisture source of precipitation in Western Dronning Maud Land, Antarctica, *Antarct. Sci.*, *13*(2), 210–220.
Reijmer, C. H., M. R. van den Broeke, and M. P. Scheele (2002), Air parcel trajectories to five deep drilling locations on Antarctica, based on the ERA-15 data set, *J. Clim.*, *15*, 1957–1968.
Revel-Rolland, M., P. De Deckker, B. Delmonte, P. P. Hesse, J. W. Magee, I. Basile-Doelsch, F. Grousset, and D. Bosch (2006), Eastern Australia: A possible source of dust in East Antarctica interglacial ice, *Earth Planet. Sci. Lett.*, *249*, 1–13, doi:10.1016/j.epsl.2006.06.028.
Röthlisberger, R., M. Bigler, M. Hutterli, S. Sommer, B. Stauffer, H. G. Junghans, and D. Wagenbach (2000), Technique for continuous high-resolution analysis of trace substances in firn and ice cores, *Environ. Sci. Technol.*, *34*, 338–342, doi:10.1021/es9907055.
Röthlisberger, R., R. Mulvaney, E. W. Wolff, M. A. Hutterli, M. Bigler, S. Sommer, and J. Jouzel (2002), Dust and sea salt variability in central East Antarctica (Dome C) over the last 45 kyrs and its implications for southern high-latitude climate, *Geophys. Res. Lett.*, *29*(20), 1963, doi:10.1029/2002GL015186.
Ruth, U., D. Wagenbach, J. P. Steffensen, and M. Bigler (2003), Continuous record of microparticle concentration and size distribution in the central Greenland NGRIP ice core during the last glacial period, *J. Geophys. Res.*, *108*(D3), 4098, doi:10.1029/2002JD002376.
Schlosser, E., K. W. Manning, J. G. Powers, M. G. Duda, G. Birnbaum, and K. Fujita (2010), Characteristics of high-precipitation events in Dronning Maud Land, Antarctica, *J. Geophys. Res.*, *115*, D14107, doi:10.1029/2009JD013410.
Sommer, S., D. Wagenbach, R. Mulvaney, and H. Fischer (2000), Glacio-chemical study spanning the past 2 kyr on three ice cores from Dronning Maud Land, Antarctica: 2. Seasonally resolved chemical records, *J. Geophys. Res.*, *105*(D24), 29,423–29,433, doi:10.1029/2000JD900450.
Stenni, B., et al. (2010), Expression of the bipolar see-saw in Antarctic climate records during the last deglaciation, *Nat. Geosci.*, *4*, 46–49, doi:10.1038/ngeo1026.

Tuncel, G., N. K. Aras, and W. H. Zoller (1989), Temporal variations and sources of elements in the Southpole atmosphere: 1. nonenriched and moderately enriched elements, *J. Geophys. Res.*, *94*(D10), 13,025–13,039, doi:10.1029/JD094iD10p13025.

Unnerstad, L., and M. Hansson (2001), Simulated airborne particle size distributions over Greenland during Last Glacial Maximum, *Geophys. Res. Lett.*, *28*(2), 287–290, doi:10.1029/2000GL012194.

Veres, D., et al. (2013), The Antarctic ice core chronology (AICC2012): An optimized multi-parameter and multi-site dating approach for the last 120 thousand years, *Clim. Past*, *9*, 1733–1748, doi:10.5194/cp-9-1733-2013.

Wegner, A., P. Gabrielli, D. Wilhelms-Dick, U. Ruth, M. Kriews, P. De Deckker, C. Barbante, G. Cozzi, B. Delmonte, and H. Fischer (2012), Change in dust variability in the Atlantic Sector of Antarctica at the end of the last deglaciation, *Clim. Past*, *8*, 135–147, doi:10.5194/cp-8-135-2012.

Welker, C., O. Martius, P. Froidevaux, C. H. Reijmer, and H. Fischer (2015), A climatological analysis of high-precipitation events in Dronning Maud Land Antarctica, and associated large-scale atmospheric conditions, *J. Geophys. Res. Atmos.*, *119*, 11,932–11,954, doi:10.1002/2014JD022259.

Weller, R., and D. Wagenbach (2007), Year-round chemical aerosol records in continental Antarctica obtained by automatic samplings, *Tellus*, *59B*, 755–765, doi:10.1111/j.1600-0889.2007.00293.x.